Associations between Afrotropical bats, parasites, and microbial symbionts

Lutz, Holly L.[1,2] *, Jackson, Elliot W.[3], Dick, Carl W.[2,4], Webala, Paul W.[5], Babyesiza, Waswa S.[6], Kerbis Peterhans, Julian C.[2,7], Demos, Terrence C.[2], Patterson, Bruce D.[2], Gilbert, Jack A.[1,8] *

[1] Department of Surgery, University of Chicago, Chicago, Illinois, USA.

[2] Integrative Research Center, Field Museum of Natural History, Chicago, Illinois, USA

[3] Department of Microbiology, Cornell University, Ithaca, New York, USA

[4] Department of Biology, Western Kentucky University, Bowling Green, Kentucky, USA

[5] Department of Forestry and Wildlife Management, Maasai Mara University, Narok, Kenya

[6] Department of Wildlife Management, Sokoine University of Agriculture, Morogoro, Tanzania

[7] Department of Biological Sciences, Roosevelt University, Chicago, Illinois, USA

[8] Biosciences Division, Argonne National Laboratory, Argonne, Illinois, USA

Corresponding author:

Holly L. Lutz & Jack A. Gilbert

Department of Surgery

Division of the Biological Sciences

University of Chicago

5851 S. Maryland Avenue

Chicago, IL 60637 - 1508
hlutz@surgery.bsd.uchicago.edu
gilbertjack@uchicago.edu

ABSTRACT

Bats are among the most diverse animals on the planet and harbor numerous bacterial, viral, and eukaryotic symbionts. The interplay between bacterial community composition and parasitism in bats is not well understood and may have important implications for studies of similar systems. Here we present a comprehensive survey of dipteran and haemosporidian parasites, and characterize the gut, oral, and skin microbiota of Afrotropical bats. We identify significant correlations between bacterial community composition of the skin and dipteran ectoparasite prevalence across four major bat lineages, as well as links between the oral microbiome and malarial parasitism, suggesting a potential mechanism for host selection and vector-borne disease transmission in bats. In contrast to recent studies of host-microbe phylosymbiosis in mammals, we find no correlation between chiropteran phylogenetic distances and bacterial community dissimilarity across the three anatomical sites, suggesting that host environment is more important than shared ancestry in shaping the composition of bat-associated bacterial communities.

Keywords: microbiome, malaria, vector-borne disease, Afrotropics, Chiroptera

SIGNIFICANCE

Animals rely on bacterial symbionts for numerous biological functions, such as digestion and immune system development. Increasing evidence suggests that host-associated microbes may play a role in mediating parasite burden. This study is the first to provide a comprehensive survey of bacterial symbionts from multiple anatomical sites across a broad taxonomic range of Afrotropical bats, demonstrating significant associations between the bat microbiome and parasite prevalence. This study provides a framework for future approaches to systems biology of host-symbiont interactions across broad taxonomic scales, emphasizing the interdependence between microbial symbionts and vertebrate health in the study of wild organisms and their natural history.

70

71 INTRODUCTION

72

73 Humans and other animals rely on bacterial symbionts for numerous biological
74 functions, such as digestion and immune system development (1, 2). Many studies have
75 found significant associations between host phylogeny (shared common ancestry) and
76 bacterial community composition (3, 4), while others have identified dietary or
77 spatiotemporal variables as significant drivers of host-microbe associations over the course
78 of an individual lifespan (5-7). The influence of microbes on their hosts may be context
79 dependent, such that the presence of a particular microbe may be beneficial under one set
80 of ecological conditions and harmful under another. Thus, patterns of association
81 between animals and bacterial symbionts provide a unique lens through which to explore
82 evolutionary and ecological phenomena.

83 Recognition of the interdependence between microbial symbionts and animal
84 health has led to a growing paradigm shift in the study of wild organisms and their
85 natural history. In addition to exhibiting variation in life history characteristics, animals
86 serve as hosts to myriad bacteria, archaea, viruses, fungi, and eukaryotic organisms. Many
87 relationships between eukaryotic parasites and hosts have ancient origins, and the same
88 may be true for host-microbial associations. It is possible that bacterial symbionts of
89 vertebrate hosts interact with eukaryotic parasites, viruses, or fungal symbionts in ways
90 that could shape host evolution (8). For example, evidence from human and
91 anthropophilic mosquito interactions suggests that the skin microbiome can influence
92 vector feeding preference, thereby affecting transmission patterns of mosquito-borne

93 pathogens (such as West Nile virus, yellow fever, dengue, malaria, etc.), and ultimately
94 imposing selective pressures on human populations - indeed, positive selection of
95 malaria-protective genes can be seen in the human genome (9). Despite the potential
96 significance of such interactions between hosts, microbes, and pathogen-transmitting
97 vectors, they have not been well studied in most wild vertebrate systems.

98 Bats (Mammalia: Chiroptera) are an important system for comparison of the
99 relative contributions of evolutionary and ecological factors driving host-symbiont
100 associations. In addition to being one of the most speciose orders of mammals (second
101 only to the order Rodentia), bats frequently live in large colonies, are long-lived, and
102 volant, granting them access to a wide geographic range relative to their non-volant
103 mammalian counterparts. The associations of diverse eukaryotic parasites (*e.g.* dipteran
104 insects, haemosporidia, helminths) within numerous bat lineages have been well-
105 characterized (10-13). Furthermore, bats have received increasing attention due to their
106 role as reservoirs of human pathogens (*e.g.* Ebola, Marburg, Nipah, SARS (14-18)).
107 Taken together, these features make bats an important and tractable model for studying
108 the interaction of bacterial symbionts and non-bacterial parasites and pathogens.

109 In this study, we conduct the first broad-scale study of Afrotropical bat-associated
110 microbes. We test associations between bacterial community composition in the
111 gastrointestinal tract, skin, and oral cavities from nine families and nineteen genera of
112 bats. We pair this information with host-parasite associations between bats and
113 ectoparasites in the superfamily Hippoboscoidea (obligate hematophagous dipteran
114 insects), and haemosporidian (malarial) parasites putatively vectored by these
115 hippoboscoid insects. Using a combination of machine learning, network theory, and

116 negative binomial distribution models, we test the hypothesis that host-associated
117 bacterial communities predict prevalence of parasitism by obligate dipteran and malarial
118 parasites.
119
120 RESULTS
121
122 1) Ectoparasite and malarial parasite prevalence among Afrotropical bats
123
124 Sampling was conducted across 20 sites in Kenya and Uganda from July-August
125 of 2016. Sites ranged from sea level to ~2500m in elevation (Fig. 1; Table S1). We
126 collected gut, oral, and skin samples for bacterial community characterization from a total
127 of 494 individual bats, comprising 9 families, 19 genera, and 28 recognized species. Bat
128 families with the greatest representation included Hipposideridae (n = 80), Miniopteridae
129 (n = 116), Rhinolophidae (n = 88), and Pteropodidae (n = 106). All host and parasite
130 vouchers are accessioned at the Field Museum of Natural History (Chicago, IL, USA)
131 (Table S2). Miniopterid bats experienced the highest prevalence of both ectoparasitism
132 (*M. minor*, 89%) and malarial parasitism (*M. minor*, 67%) (Table 1). Bats with similarly
133 high ectoparasite prevalence at the host species level included *Rhinolophus eloquens* (79%
134 prevalence), *Stenonycteris lanosus* (62%), and *Triaenops afer* (60%). Unlike miniopterid
135 bats, these bat species did not harbor any detectable malarial parasites (Table 1).
136
137
138

Table 1. Bat sampling, ectoparasite prevalence (n_{ecto}), and malarial parasite prevalence (n_{haem}) and identification.

Bat family	Bat species	n_{bats}	n_{ecto} (%)	n_{haem} (%)
Emballonuridae	*Coleura afra*	11	2 (18)	0
Hipposideridae	*Hipposideros caffer*	47	18 (38)	0
	Hipposideros camerunensis	1	0	0
	Hipposideros ruber	21	16 (76)	0
	Macronycteris vittatus	10	0	0
Miniopteridae	*Miniopterus africanus*	22	13 (59)	11 (50)
	Miniopterus natalensis	54	16 (30)	13 (24)
	Miniopterus rufus	22	20 (61)	20 (91)
	Miniopterus minor	18	16 (89)	12 (67)
Molossidae	*Chaerephon bivittatus*	14	0	0
	Otomops harrisoni	33	1 (3)	0
Nycteridae	*Nycteris arge*	3	0	0
	Nycteris thebaica	7	1 (14)	0
	Nycteris sp.	6	0	0
Pteropodidae	*Epomophorus labiatus*	2	0	0
	Epomophorus wahlbergi	11	0	3 (27)
	Micropteropus pusillus	4	0	0
	Myonycteris angolensis	5	0	0
	Rousettus aegyptiacus	47	24 (50)	0
	Stenonycteris lanosus	37	23 (62)	0
Rhinolophidae	*Rhinolophus clivosus*	43	8 (19)	0
	Rhinolophus eloquens	24	19 (79)	0
	Rhinolophus hildebrandti	4	1 (25)	0
	Rhinolophus landeri	14	0	3 (21)
	Rhinolophus sp.	3	0	
Rhinonycteridae	*Triaenops afer*	10	6 (60)	0
Vespertilionidae	*Myotis tricolor*	9	8 (89)	3 (33)
	Neoromicia nana	1	0	0
	Neoromicia sp.	3	0	
	Pipistrellus sp.	2	0	0
	Scotoecus hindei	3	1 (25)	0
	Scotophilus dinganii	3	0	0
Total		494	193	65

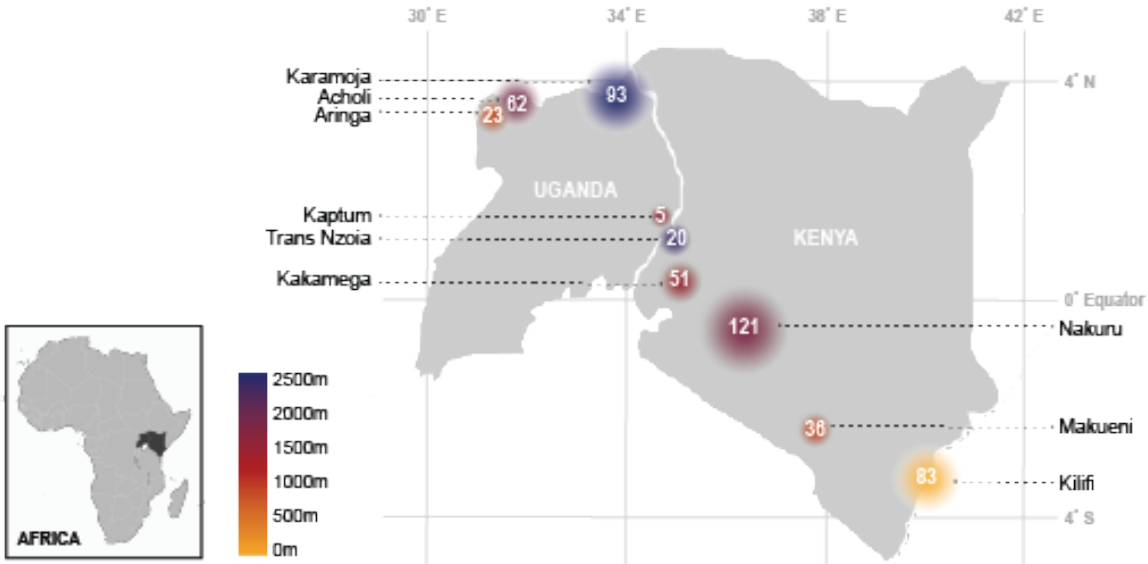

Figure 1. Sampling localities and elevation, grouped by county (see Table S1 for full locality information). Colors correspond to elevation, and white numbers and size of points correspond to number of bats collected.

2) Microbial richness associated with bat skin is significantly greater than gut or oral microbial communities

Sequencing produced a total of 1,236 libraries, with an average read depth of 32,950 reads per library (±19,850 reads). Analyses and statistical tests were performed on non-rarefied data (libraries containing >1000 reads and transformed to library read depth) and on rarefied data (libraries rarefied to a read depth of 10,000 sequences and subsequently transformed). The difference in library normalization methods only resulted in a decrease of total ASVs which did not affect the significance of alpha and beta-diversity statistical tests. Therefore, the results reported hereafter are from the non-

rarefied data set. Across all samples, 31,172 amplicon sequence variants (ASVs) were identified using Deblur (19) (for rarefied data set, 1,267 ASVs were dropped, resulting in a total of 29,890 ASVs identified across all samples). Total number of libraries per anatomical site, following filtering, included 396 libraries for gut, 374 libraries for oral, and 458 libraries for skin microbiomes (Table 2). Gut microbial communities exhibited the lowest overall diversity (8,204 ASVs), followed by oral (11,632 ASVs), and skin (29,149 ASVs), the latter being significantly greater than gut or oral (p < 2.2e-16, Kruskal-Wallis; Bonferroni corrected p-value p < 1e-113, Dunn's test) (Fig. 2; Fig S1). The mean observed ASVs by anatomical site were 69, 96, and 587 for gut, oral, and skin samples, respectively (Table 2). Shannon index score of skin microbial communities were also significantly greater than gut or oral microbial communities (p < 2.2e-16, Kruskal-Wallis; Bonferroni corrected p-value p < 1e-119, Dunn's Test) (Fig. 2; Fig. S1).

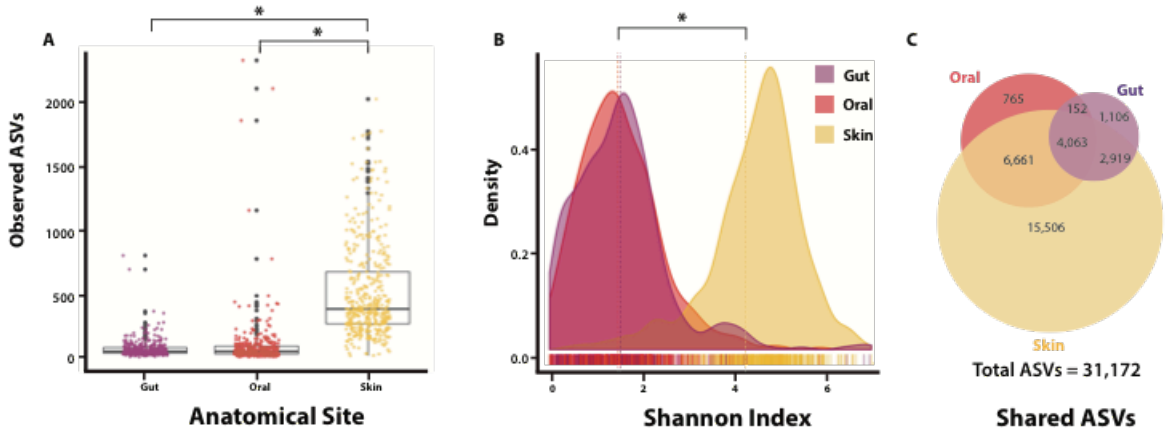

Figure 2. Alpha diversity of amplicon sequence variants (ASVs) by anatomical sites, including (A) Observed richness, (B) Shannon index of diversity, (C) ASVs shared between anatomical sites. Asterisks indicate significant differences between groups (Dunn's Test, Bonferroni corrected p-value p < 0.0001).

Table 2. Alpha diversity of microbial communities across anatomical sites within each host genus, measured by Shannon Index of diversity (SI) and observed ASV richness (obs); n corresponds to number of libraries included in each calculation (following quality filtering).

		Fecal			Oral			Skin		
Host Family	Host Genus	SI	obs	n_{fecal}	SI	obs	n_{oral}	SI	obs	n_{skin}
Emballonuridae	*Chaerephon*	1.16	52	12	1.39	57	14	3.57	547	14
Hipposideridae	*Hipposideros*	1.70	79	65	2.01	155	52	4.95	439	74
	Macronycteris	1.82	74	9	2.12	110	9	4.94	883	7
Miniopteridae	*Miniopterus*	1.41	70	92	1.55	87	74	4.12	403	114
Molossidae	*Coleura*	1.59	52	11	0.38	41	11	4.01	566	11
	Otomops	0.88	53	26	0.35	22	26	3.88	288	33
Nycteridae	*Nycteris*	1.60	80	10	1.62	78	14	4.48	807	14
Pteropodidae	*Epomophorus*	1.44	49	11	1.42	46	11	3.78	566	13
	Micropteropus	1.90	39	3	2.21	39	4	2.30	84	3
	Myonycteris	1.14	117	4	1.29	195	5	5.21	1246	4
	Rousettus	1.62	93	32	1.95	84	34	4.90	1207	34
	Stenonycteris	1.55	61	41	1.72	97	38	4.59	855	33
Rhinolophidae	*Rhinolophus*	1.34	62	58	1.95	81	59	4.71	543	79
Rhinonycteridae	*Triaenops*	1.69	82	9	1.28	414	9	4.03	508	10
Vespertilionidae	*Myotis*	1.62	54	1	1.33	72	6	5.41	771	3
	Neoromicia	2.13	65	4	1.47	37	4	3.76	267	4
	Pipistrellus	1.05	NA	1	NA	NA	0	4.80	360	2
	Scotoecus	1.86	92	4	1.97	17	3	4.20	360	4
	Scotophilus	1.23	64	3	0.38	96	1	4.08	459	2
				n_{fecal}			n_{orall}			n_{skin}
Mean		1.51	69	396	1.47	96	374	4.30	587	458

3) Microbial communities significantly correlate with geographic locality, anatomical site, and host taxonomy, but not host phylogeny

Permutational analysis of variance (PERMANOVA) identified geographic locality, host taxonomy, and anatomical sampling site (gut, oral, skin) as significant factors explaining variation in three independent measures of microbial beta diversity (Bray-Curtis, unweighted UniFrac, and weighted UniFrac) ($p < 0.001$, ADONIS) (Table

189 3). Measures of intraspecific beta dispersion among weighted UniFrac, unweighted
190 UniFrac, and Bray-Curtis distances showed a continuum of dissimilarities across host
191 species (Fig. S2); mean beta dispersion differed significantly between anatomical sites by
192 all three dissimilarity measures (Dunn's Test, Bonferroni corrected p-value $p < 0.001$).)
193 Analysis of sites by elevation revealed that bats at higher elevations tended to host
194 increased Shannon diversity (SI) and observed richness (OR) across oral (SI: $R^2 = 0.076$,
195 $p < 3.1e-9$; OR: $R^2 = 0.038$, $p < 2.5e-5$), and skin (SI: $R^2 = 0.16$, $p < 2.2e-16$; OR: $R^2 =$
196 0.100, $p < 2.5e-14$) microbiomes (Fig. S3).
197 Across all bat species, the gut microbiome was enriched for Proteobacteria (avg
198 55.4%) (Enterobacteraceae, avg 50.0%) and Firmicutes (avg 21%) (Clostridiaceae, avg
199 9.5%; Streptococcaceae, avg 5.5%). Oral microbiota were also enriched for Proteobacteria
200 (avg 64.3%) (Pasteurellaceae, avg 47.5%; Neisseriaceae, avg 8.3%) and Firmicutes (avg
201 11.4%) (Streptoccaceae, avg 8.8%; Gemellaceae, avg 3.61%). The skin microbiome was
202 not enriched for a single bacterial family, and showed a pronounced increase in relative
203 abundance of Actinobacteria (avg 10%) (Mycobacteraceae, avg 4.1%;
204 Pseudonocardiaceae, avg 2.8%; Nocardiaceae, avg 2.3%) and Bacteroidetes
205 (Moraxellaceae, avg 5.6%), and Euryarchaeota (Halobacteraceae, avg 4.2%) (Fig. 3).
206 Fruit bats (pteropodids) showed enrichment of Clostridiaceae in the gut (avg
207 24.8%) and Streptococcaeae in the oral microbiome (avg 31.0%) compared to all other
208 bats. The oral microbiota of several insectivorous bat families were enriched for
209 Firmicutes in the Mycoplasmataceae family (nycterids, avg 25.5% ; rhinolophids, avg
210 13.8%; miniopterids, avg 8.4%). The skin microbiota of several insectivorous bat families

were enriched for Firmicutes in the Bacillaceae family (molossids, 14.0%; hipposiderids, 8.6%; nycterids, 8.6%; rhinolophids, 6.3%).

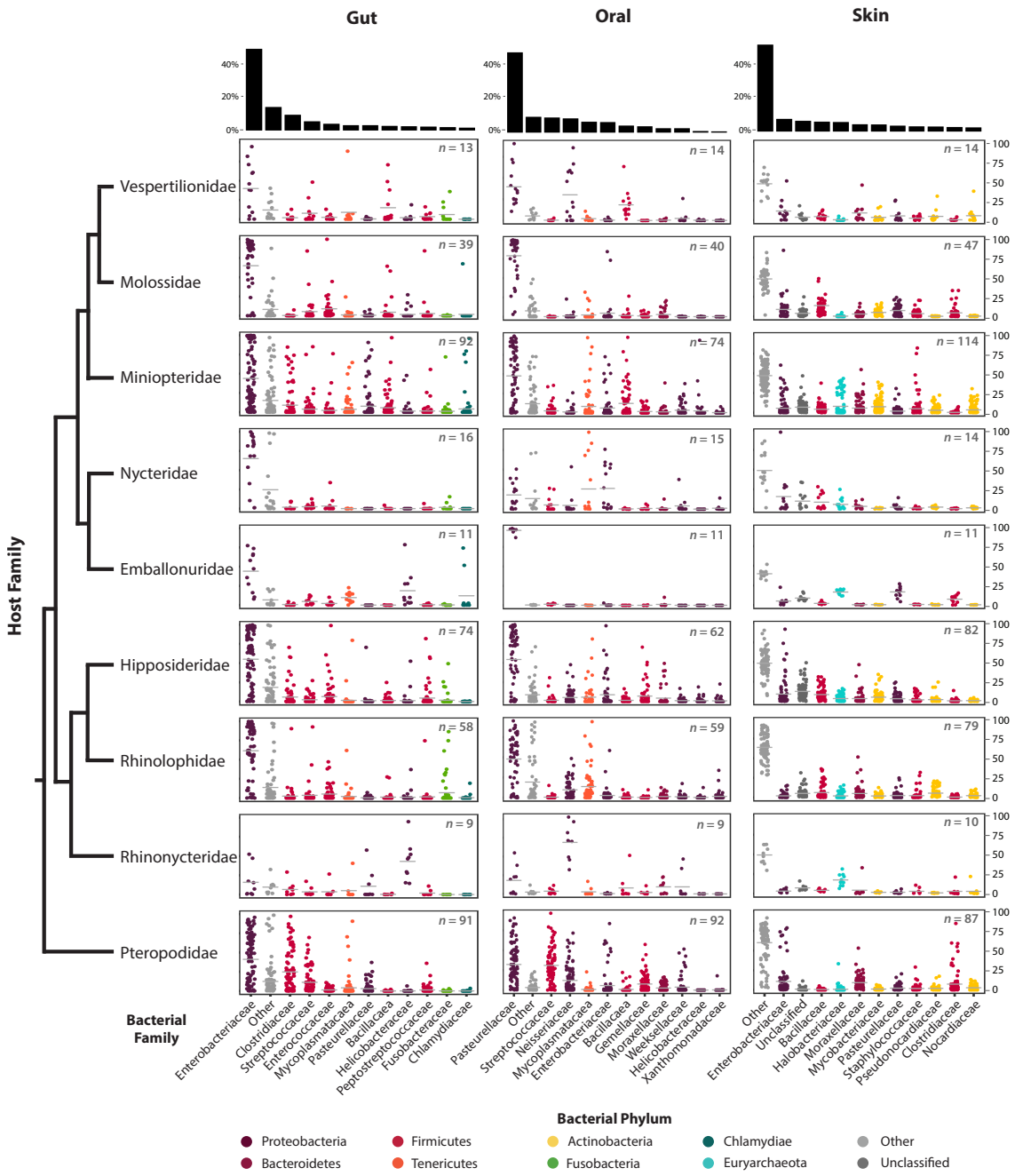

Figure 3. Relative abundance of top 11 bacterial families identified in gut, oral, and skin microniomes of bats. Individual points correspond to libraries. Bacterial families are

colored according to bacterial phylum. Number of libraries is indicated in the upper right-hand corner of each plot. Black bar graphs indicate average relative abundances.

Host phylogeny from bat specimens collected during this study was reconstructed to test for significance of phylosymbiosis between bat species and their microbiome (Supplemental Figure 5; Figure 4). Mantel tests of host phylogenetic distances and microbial community dissimilarity (weighted (wuf) and unweighted UniFrac (uf) distances) revealed no correlation for gut (wuf: R^2 = - 0.045, p = 0.63; uf: R^2 = - 0.052, p = 0.64), oral (wuf: R^2 = - 0.11, p = 0.88), and skin (wuf: R^2 = - 0.081, p = 0.79; uf: R^2 = - 0.108, p = 0.92) microbiota and host phylogenetic distance, with the exception of oral uf dissimilarity and host phylogenetic distance(uf: R^2 = 0.223, p = 0.02) (Fig. 4).

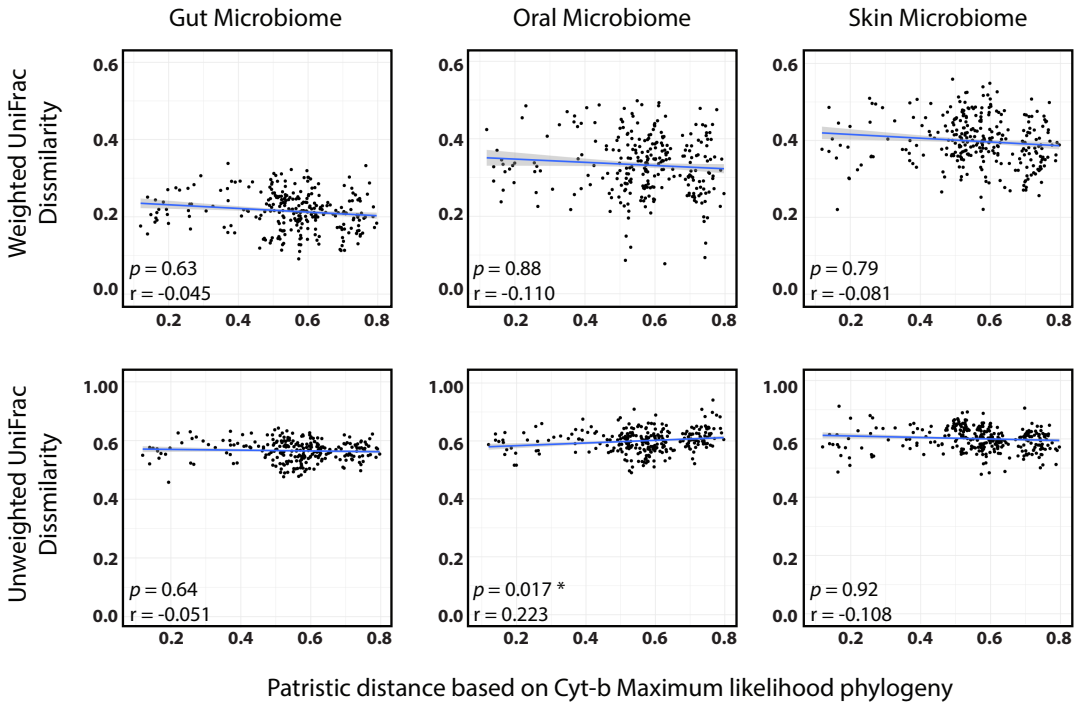

228 Figure 4. Rate of microbiome divergence across phylogenetic distance of bats. Strengths of
229 correlations assessed by Mantel tests (10,000 permutations) of microbial community
230 dissimilarity (unweighted and weighted UniFrac) and patristic distances calculated from a
231 maximum likelihood hypothesis of bat species from this study. Asterisk indicates significant
232 correlation ($p<0.05$) as determined by Mantel test.
233
234 4) Bat skin microbiome is associated with parasitism in African bats
235
236 To test for significant associations between bacterial communities and eukaryotic
237 parasites (obligate ectoparasitic dipteran insects, and obligate endoparasitic malarial
238 parasites), we employed a combination of machine learning techniques, network analyses,
239 and DESeq2 models (see methods). PERMANOVA analysis identified ectoparasite
240 status and malarial infection status as significant predictors of bacterial beta diversity
241 dissimilarity among skin and oral microbiota, respectively ($p < 0.001$, ADONIS). Tests of
242 three independent measures of beta diversity (weighted UniFrac, unweighted UniFrac,
243 and Bray-Curtis) produced congruent results, with the exception of oral microbiome,
244 which was not significantly predictive of malarial infection based on unweighted UniFrac
245 analysis (Table 4).
246
247
248
249

250 Table 4. Permutational multivariate analysis of variance using distance matrices, with distance matrices
251 among sources of variation partitioned by host taxonomy (species nested within genus), ectoparasite
252 status, malarial infection status, and locality included as strata; * indicates p-value < 0.05.
253
254

		Weighted UniFrac			Unweighted UniFrac			Bray-Curtis		
Site	Partition Variable	F	R2	Pr(>F)	F	R2	Pr(>F)	F	R2	Pr(>F)
Fecal	(Host genus (species))	4.27	0.162	0.001*	3.15	0.120	0.001*	2.89	0.110	0.001*
	Ectoparasite status	0.47	0.001	0.912	1.42	0.004	0.048*	1.40	0.004	0.097
	Malarial status	1.34	0.004	0.21	1.33	0.004	0.077	1.98	0.005	0.011*
Oral	(Host genus (species))	6.82	0.279	0.001*	3.50	0.143	0.001*	6.69	0.274	0.001*
	Ectoparasite status	0.51	0.001	0.836	1.41	0.004	0.057	1.00	0.003	0.447
	Malarial status	2.78	0.008	0.015*	1.17	0.003	0.2	1.98	0.006	0.019*
Skin	(Host genus (species))	7.68	0.329	0.001*	3.98	0.170	0.001*	5.60	0.240	0.001*
	Ectoparasite status	2.42	0.006	0.01*	1.54	0.004	0.02*	2.07	0.005	0.001*
	Malarial status	0.92	0.002	0.513	1.02	0.002	0.363	1.06	0.003	0.32

255
256

257 Supervised machine learning analyses (random forests) produced models that
258 could classify the anatomical source of microbial communities and the host genus of gut,
259 oral, and skin microbial samples with reasonable accuracy (ratio of baseline to observed
260 classification error ≥2; *i.e.* random forest models performed at least twice as well as
261 random). Random forest models also performed accurately when classifying ectoparasite
262 status based on skin bacterial community composition, but were less accurate for
263 classification of malarial status based on oral bacterial community composition (Table 5).
264
265
266
267

Table 5. Supervised machine learning results, showing random forest model performance with respect to different classification variables and input data sets (fecal, oral, skin microbiome). Model performance is assessed by measuring the ratio of Out-of-bag estimated error (OOB) to baseline error.

Classification variable	Input Data	Baseline error	OOB error	Baseline:OOB
Anatomical site	All data	0.68	0.14	4.8
Host Genus	Skin	0.75	0.17	4.3
Host Genus	Oral	0.78	0.24	3.2
Host Genus	Gut	0.77	0.35	2.2
Ectoparasite Status	Skin	0.53	0.27	2.0
Malarial Status (Miniopteridae only)	Oral	0.46	0.38	1.2

Following the application of statistical and machine learning approaches, we employed network analyses to characterize the co-occurrence topology of microbial communities (in terms of the relative abundance of co-occurring ASVs) across the skin microbiota of our four most well-sampled bat families (Hipposideridae (n = 80), Miniopteridae (n = 116), Rhinolophida (n = 88), and Pteropodidae (n = 106)). Network analyses produced strikingly consistent results, revealing a significant decrease in cluster size ($p < 0.05$, Mann-Whitney-Wilcoxon rank sum test) and median node degree ($p < 0.05$, t test), as well as reduced network connectivity for parasitized bats from three of the four bat families examined (Fig. 5; Fig. S4).

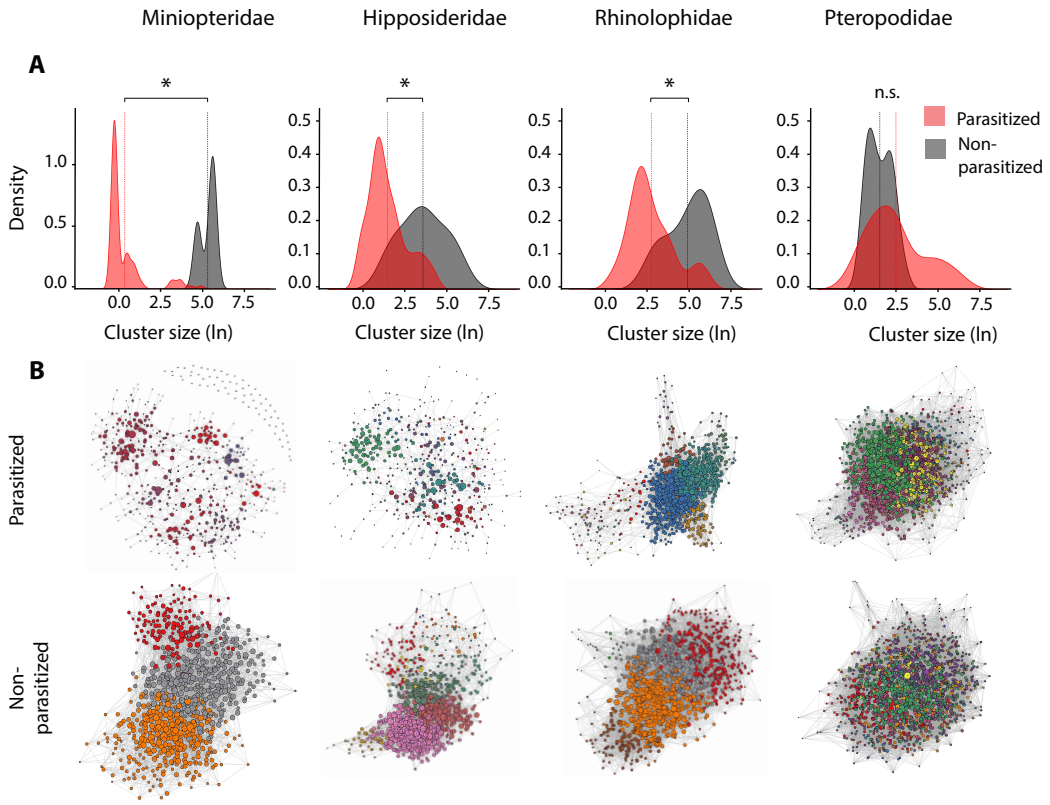

Figure 5. (A) Distribution of skin microbial network clusters for parasitized and non-parasitized bats, grouped by bat family (asterisks indicate signifiance at $p < 0.005$, Kruskal-Wallis) (B) Visualization of skin bacterial networks (based on Fruchterman-Reingold algorithm); colored nodes correspond to unique clusters of co-occurring ASVs within each network.

5) Bacterial taxa on skin correlated with presence or absence of obligate dipteran ectoparasites

DESeq2 analyses of the skin microbiota in four well-sampled bat families (Hipposideridae, Miniopteridae, Rhinolophidae, Pteropodidae) identified a number of

295 ASVs that were significantly associated with either ectoparasitized or non-ectoparasitized
296 bats (Fig. 6). Overall, we identified 89 and 24 ASVs significantly associated with
297 parasitized and non-parasitized bats, respectively (Table S3). Bacterial classes with the
298 greatest representation among significant results were Actinobacteria (16 families),
299 Gammaproteobacteria (11 families), Bacilli (5 families), and Alphaproteobacteria (3
300 families). ASVs significantly enriched in parasitized bats from at least three out of four
301 bat families included Mycobacteraceae (Actinobacteria), and Xanthomonadaceae
302 (Gammaproteobacteria). ASVs significantly enriched in parasitized bats from at least two
303 out of four bat families included Hyphomicrobiaceae (Alphaproteobacteria),
304 Alcaligenaceae (Betaproteobacteria), Moraxellaceae (Gammaproteobacteria),
305 Planococcaceae (Bacilli), Flavobacteraceae (Flavobacteria), Halobacteraceae
306 (Halobacteria), and Chitinophagaceae (Saprospirae) (Fig. 6).

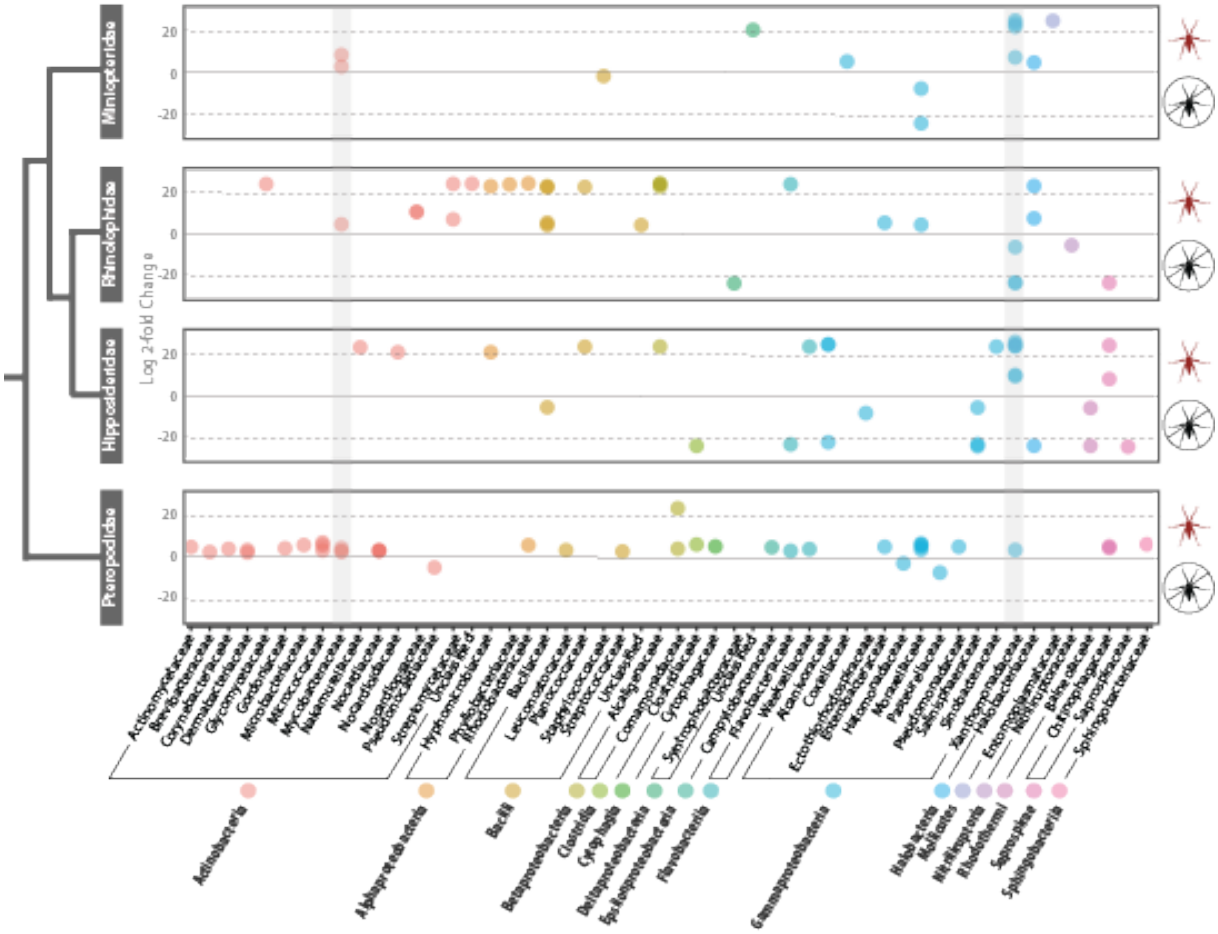

Figure 6. Log2fold change in relative abundance of skin-associated ASVs from the four most-sampled bat families estimated with DESeq2. ASVs shown were found to be significantly associated with ectoparasite status in bats based on analysis of negative binomial distributions of relative abundance (Banjamini-Hochberg FDR corrected *p*-value $p < 0.05$). Positive values correspond to ASVs found to be enriched on parasitized bats, and negative values correspond to ASVs found to be enriched on non-parasitized bats. Gray bars highlight ASVs in bacterial families that were enriched in parasitized bats for three out of four bat families.

DISCUSSION

The bacterial diversity we observed among gut, oral, and skin microbiota of bats fall within ranges similarly observed in other vertebrate groups (3, 20-23). Although few studies have simultaneously compared gut, oral, and skin microbiota from the same individuals, our data reflect an apparent trend in the literature of skin bacterial diversity among vertebrates significantly outnumbering gut or oral bacterial diversity (24-27). Our data corroborate the findings of Nishida and Ochman (3), revealing no relationship between chiropteran phylogeny and gut bacterial community dissimilarity. We also found the same absence of phylogenetic signal among oral and skin microbial communities. As suggested in other studies of volant vertebrates (bats and birds), convergent adaptations driven by the evolution of flight may be influencing the nature and composition of microbial communities in both bats and birds (28-30). This differs markedly from studies of other non-volant mammals, such as primates and rodents, for which phylogenetic relatedness is generally a significant predictor of microbial community dissimilarity (21, 31-33).

Microbial community specificity can be assessed as a function of intraspecific variation in dissimilarity (beta dispersion), where a low variance of dispersion suggests a tight and perhaps co-evolutionary link between hosts and symbionts, and a high variance of dispersion suggests more random or non-specific associations between hosts and symbionts (34). Measures of beta dispersion among bat species revealed a continuum for all three anatomical sites, with oral bacterial communities showing lower levels of beta dispersion than gut or skin communities (Fig. S2). Given that we found no correlation

341 between bacterial community dissimilarity and host phylogenetic distance, and that we
342 observed no taxonomic clustering of hosts in mean beta dispersion estimates, variation in
343 beta dispersion is likely driven by ecological rather than evolutionary factors.

344 Similar to recent studies in North American bats (35), we found sampling locality
345 to be a significant factor influencing skin, gut and oral microbial composition (Table 3).
346 Furthermore, we observed an apparent trend in increasing Shannon diversity and
347 observed ASV richness along an elevational gradient that was most pronounced for skin
348 microbiota (Fig. S3). A positive correlation between bacterial richness and elevation has
349 been observed in studies of amphibian skin (36) and montane soil, and this pattern may
350 be the result of climatological and other abiotic factors (*e.g.* pH) found along elevational
351 gradients (37, 38).

352 Table 3. Permutational multivariate analysis of variance using distance matrices, with distance matrices
353 among sources of variation partitioned by host taxonomy (species nested within genus), locality, and
354 anatomical site; * indicates p-value < 0.05.
355
356

	Weighted UniFrac			Unweighted UniFrac			Bray-Curtis		
Partition Variable	SumSq	F	Pr(>F)	SumSq	F	Pr(>F)	SumSq	F	Pr(>F)
Anatomical site	10.67	198.01	0.001*	56.52	82.90	0.001*	38.2	36.97	0.001*
Host Genus	3.77	13.09	0.001*	25.54	7.02	0.001*	85.30	15.06	0.001*
Locality	1.56	11.00	0.001*	20.62	11.34	0.001*	23.85	8.42	0.001*
Host Genus:species	1.39	4.08	0.001*	11.20	2.59	0.001*	25.25	1.33	0.001*

357
358

359 We found the general composition of gut microbiota in East African bats to be
360 similar to that of Neotropical bats, with Proteobacteria being the dominant bacterial
361 phylum present (39). Regardless of diet (insectivorous or frugivorous), the distal bat gut is
362 dominated by bacteria in the family Enterobacteriaceae (Phylum: Proteobacteria), though

363 fruit bats do have an increased relative abundance of bacteria in the family Clostridiaceae
364 (Phylum: Firmicutes) relative to insectivorous bats. In their study of neotropical bats,
365 Phillips et al. (40) noted an increased relative abundance of Lactobacillales in frugivorous
366 bats, and we note a similar pattern among pteropodid fruit bats in this study, which
367 exhibited a slightly higher proportion of Streptococcaceae (Order: Lactobacillales)
368 relative to insectivorous bats (Fig. 3). Overall, the predominant enrichment of the
369 chiropteran gut by Proteobacteria differs markedly from other mammalian gut
370 microbiomes, which are generally dominated by Firmicutes (21, 41, 42).

371 Among most bat families, the oral microbiome was dominated by Pasteurellaceae
372 (Phylum: Proteobacteria), and in some cases a high relative abundance of bacteria in the
373 families Mycoplasmataceae (in nycterids), Neisseriaceae (in vespertilionids and
374 rhinonycterids), and Streptococcaceae (in pteropodids) was also observed. Although the
375 oral microbiome has received less attention than that of the gut, several studies have
376 found diverse Pasteurellaceae and Neiserria lineages present in the oral microbiota of
377 animals, including domestic cats (20) and marine mammals (43). Pasteurellaceae lineages
378 have also recently been documented in the oral microbiota of Tasmanian devils (23, 44).
379 In humans, Pasteurallaceae (genera *Haemophilus* and *Aggregatibacter*) and Neisseriaceae
380 (genera *Neisseria*, *Kingella*, and *Eikenella*) play an important role in the formation
381 supragingival plaque (22). Though these bacterial groups are present in lower proportions
382 in other animals relative to bats, their presence in a broad range of host taxa suggest a
383 conserved evolutionary niche.

384 Our analysis identified links between ectoparasitism, malarial parasitism, and
385 bacterial communities on the skin and in oral cavities, respectively. Network analyses

386 identified consistent, stable, and species-rich clusters of bacteria on the skin of non-
387 ectoparasitized bats, compared to relatively disconnected and apparently transient bacteria
388 on the skin of bats harboring ectoparasites. This result mirrors that found in human-
389 mosquito interactions, in which individuals with lower bacterial diversity on the skin are
390 significantly more attractive to blood-seeking mosquitoes than individuals with higher
391 diversity (45). In humans, skin bacteria play a known role in attracting mosquitoes via
392 their production of volatile organic compounds (VOCs), and studies have shown that
393 variation in skin microbial community composition can increase or decrease human
394 attractiveness to blood-seeking mosquitoes (45-47). Similar mechanisms may be at play
395 in the bat-ectoparasite system, particularly given the phylogenetic proximity of
396 hippobscoid bat parasites to mosquitoes.

397 Several bacterial families exhibited significant associations with presence of
398 ectoparasitism in bats based on DESeq analyses. Bacteria found across multiple host
399 families included (but were not limited to) Alcaligenaceae, Chitinophagaceae,
400 Flavobacteriaceae, Moraxellaceae, Mycobacteriaceae (*Mycobacterium* spp.), and
401 Xanthomonadaceae. In many cases, these bacterial families were associated with
402 parasitism in some bat families, and absence of parasitism in others, suggesting a
403 potential mechanism by which ectoparasites might be distinguishing between "correct"
404 and "incorrect" hosts. As suggested by human-mosquito interaction studies (45, 46, 48),
405 bacteria positively associated with increased rates of blood-feeding dipteran host selection
406 may be producing VOCs on which the insects rely to identify their hosts. Bacteria that
407 are negatively associated with such insects may be consuming the products of the former,
408 or may be producing VOCs of their own that mask those of the former (suggested by

409 Verhulst et al. (45)). To better understand the mechanisms underlying these correlations
410 in wild populations, future experiments should consider including sampling of VOCs *in*
411 *vivo*.

412 PERMANOVA analyses identified associations between the oral microbiome
413 and malarial parasite prevalence among bats in the family Miniopteridae, although these
414 associations were less robust than those of the skin bacteria and ectoparasitism. Upon
415 further exploration of this potential association, we identified a single bacterial ASV in
416 the genus *Actinobacillus* (99% similar to *A. porcinus* based on NCBI blastn search) as
417 significantly reduced in malaria-free bats (baseMean 7.61, -24.2 log2FoldChange, p =
418 1.7E-20). Network analyses indicated no significant differences in connectivity or node
419 degree distribution (results not shown). Because no other bat groups experienced rates of
420 malarial parasitism adequate for statistical analyses, we were unable to explore this
421 relationship further. Future studies that incorporate greater sampling of malaria-positive
422 species may reveal more robust microbial associations, as have been documented in
423 numerous experiments with controlled rodent and human malaria infections (48-50).

424 Although we cannot ascertain causality of differences in the microbial
425 composition of skin in this study, our results support the hypothesis that these differences
426 suggest a mechanism by which ectoparasites can locate or distinguish hosts. Alternatively,
427 observed differences in microbial composition could result from microbial transfer from
428 parasites to hosts. Given the known effect of locality and apparent absence of host
429 phylogenetic signal in microbial community composition of skin, one possible
430 explanation is that local environmental variables play a greater role in determining host-
431 bacteria associations in bats. Indeed, in North America, multiple bat species have been

432 found to share many bacterial genera with soil and plant material (35). Thus, local
433 conditions and bacterial composition of bat roosts are likely playing an important role in
434 driving the composition of skin bacteria of bats.
435
436 METHODS
437
438 1) Sampling
439
440 Sampling for this study was conducted from the eastern coast of Kenya to the northern
441 border of Uganda during August-October 2016 (Fig. 1; Table S1, S2). Nine families and
442 nineteen genera of bats (order: Chiroptera) were collected as part of bird and small
443 mammal biodiversity inventories. All sampling was conducted in accordiance with the
444 Field Museum of Natural History IACUC and voucher specimens are accessioned at the
445 Field Museum of Natural History (Table S2). Blood samples were collected and screened
446 for haemosporidia, and haemosporidian taxonomy was assigned using previously
447 described molecular methods (13). Following blood sampling, ectoparasites were
448 removed with forceps and placed directly into 95% EtOH; ectoparasites taxonomy was
449 assigned based on morphological features. For the purposes of analysis with microbiome
450 data, ectoparasite and malarial status were each scored separately as 1 (present) or 0
451 (absent). Gut, skin, and oral samples were taken for each bat for microbial analyses. Gut
452 samples consisted of fecal material collected directly from the distal end of the colon
453 using sterilized tools, and preserved on Whatman® FTA® cards for microbiome analyses.
454 For oral microbiome analyses, we preserved both buccal swabs in lN_2 and tongue biopsies

455 in 95% ethanol (EtOH). Comparison of ASV diversity obtained from paired subsets of
456 each sample type revealed greater diversity recovered from tongue biopsies (data not
457 shown); tongues were therefore used for characterization of oral microbiomes in this
458 study. Lastly, skin samples from five regions of the body (ear, wing membrane, tail
459 membrane, chest, back) were collected and pooled in 95% EtOH using sterile Integra®
460 Miltex® 5mm biopsy punches. The goal of sampling from five body regions was to
461 maximize bacterial diversity recovered from the external skin surface of each individual.
462 We based our storage media selections on the recent study by Song et al. (51).
463
464 2) Microbiome sequencing, characterization, and parasite association
465
466 DNA extractions were performed on gut, tongue, and skin samples using the MoBio
467 PowerSoil 96 Well Soil DNA Isolation Kit (Catalog No. 12955-4, MoBio, Carlsbad,
468 CA, USA). We used the standard 515f and 806r primers (52-54) to amplify the V4
469 region of the 16S rRNA gene, using mitochondrial blockers to reduce amplification of
470 host mitochondrial DNA. Sequencing was performed using paired-end 150 base reads
471 on an Illumina HiSeq sequencing platform. Following standard demultiplexing and
472 quality filtering using the Quantative Insights Into Microbial Ecology pipeline
473 (QIIME2) (55) and vsearch8.1 (56), ASVs were identified using the Deblur method (19)
474 and taxonomy was assigned using the Greengenes Database (May 2013 release;
475 http://greengenes.lbl.gov). According to a recent stuy by McMurdie and Holmes (57),
476 rarefying 16s data is inappropriate for the detection of differentially abundant species.
477 However, for the purposes of comparison, we compared both libraries rarefied to a read

478 depth of 10,000 reads and libraries filtered to those containined >1000 reads (negative
479 controls all contained fewer than 1000 reads and were filtered at this step). Alpha and
480 beta-diversity analyses produced statistically similar results, with no significant differences
481 observed betweeh the rarefied and non-rarefied data. We thus chose to report results of
482 non-rarefied data, based on these observations and the recommendation of McMurdie
483 and Holmes (57).. Following filtering, data were subset for analyses according to sample
484 type, host genus, and locality (or some combination thereof). Site-specific analyses were
485 only performed for sites from which five or more individual bats were sampled. We
486 calculated alpha diversity for each sample type (gut, oral, skin) using the Shannon index,
487 and measured species richness based on actual observed diversity. Significance of differing
488 mean values for each diversity calculation was determined using the Kruskal-Wallis rank
489 sum test, followed by a post-hoc Dunn test with bonferroni corrected *p*-values. Three
490 measures of beta diversity (unweighted UniFrac, weighted UniFrac, and Bray-Curtis)
491 were calculated using relative abundances of each ASV (calculated as ASV read depth
492 over total read depth per library). Significant drivers of communitity similarity were
493 identified using the ADONIS test with Bonferroni correction for multiple comparisons
494 using the R package Phyloseq (58). To assess potential effect of imbalanced sampling, the
495 ADONIS test was re-run on a subset of data comprising only data from the top four
496 sampled bat families, which represented even sampling among families and across the
497 localities from which they were collected. Results of this test (not reported) indicated the
498 same significant drivers of community similarity as the test run on the entire data set.

499 Additional R packages used for analyses and figure generation included vegan (59),
500 ggplot2(60), and dplyr(61). For a complete list of packages and code for microbiome
501 analyses, see http://github.com/hollylutz/BatMP.
502
503 3) Bat phylogenetic reconstruction
504
505 DNA from bats collected during this study was extracted and sequenced for
506 mitochondrial Cytochrome-*b* (cyt-*b*), using the primer pair LGL 765F and LGL 766R
507 that amplify the entire cyt-*b* gene (Bickham et al. 1995, 2004). DNA extractions, PCR
508 amplification, and sequencing were carried out as in Demos et al. 2018. The best-
509 supported model of nucleotide substitution for cyt-*b* was determined using the BIC on the
510 maximum-likelihood topology estimated independently for each model in
511 jMODELTEST2 (Darriba et al., 2012) on CIPRES Science Gateway v.3.1 (Miller et al.,
512 2010). Maximum-likelihood estimates of cyt-*b* gene trees were made using the program
513 IQ-TREE version 1.6.0 (Nguyen et al. 2017) on the CIPRES portal. Emballonuridae
514 (*Coleura afra*) was constrained as sister to Nycteridae (*Nycteris arge*, *N. thebaica*;
515 Amador et al. 2016). We conducted analyses using the ultrafast bootstrap algorithm and
516 searched for best-scoring ML tree algorithm under the GTR+I+ FreeRate model with
517 1000 bootstrap replicates. The resulting phylogenetic hypothesis and node support can be
518 viewed in Fig. S5.
519
520 4) Machine learning and network analyses
521

522 A supervised machine learning approach was used to produce random forests (RF) for the
523 classification of different variables. RFs were constructed using 1000 decision trees and
524 subsets of ASV data via the supervised_learning.py script implemented in QIIME (55),
525 which utilized 80% of each input data set to train classification models, and tested the
526 accuracy of the models on the remaining 20% of data. We tested the ability of RFs to
527 accurately classify 1) anatomical site (using all data), 2) host genus (using gut, oral, or
528 skin microbial data separately), 3) ecotparasite status (using skin microbial data), and 4)
529 malarial status (using oral microbial data). Classification categories comprised
530 approximately equal numbers of samples, with the exception of host genera, which varied
531 substantially (see Table 1). RF performance was assessed by comparing the out-of-bag
532 estimated error (OOB) with baseline (random) error. If the ratio of OOB to baseline
533 error was less than or equal to two, the model was considered to perform reasonably well,
534 as it performed at least twice as well as random (62). To reconstruct microbial networks
535 for skin and oral bacterial communities within bat family groupings (which were further
536 sub-divided into parasitized or non-parasitized), we utilized the R package Sparse Inverse
537 Covariance Estimation for Ecological Association Inference (SPIEC-EASI) (63). All
538 network datasets were filtered to contain only ASVs that appeared in at least three
539 individuals within each respective dataset. We used the neighborhood selection
540 framework (MB method) with 20 repetitions. Network results produced with SPIEC-
541 EASI were summarized using the R packages CAVnet (64) and igraph (65). Network
542 stability was assessed by sequentially removing network nodes (ordered by betweeness
543 centrality and degree) and observing natural connectivity (*i.e.* eigenvalue of the graph
544 adjacency matrix) as nodes are removed. To determine which, if any, bacterial ASVs were

545 significantly associated with ectoparasite or malarial prevalence, we performed analyses
546 based on the negative binomial distribution of ASVs relative abundance, utilizing the R
547 package DESeq2 (66). For ectoparasite-assocation tests, the data were subset into four
548 categories that corresponded to the top-sampled bat families (Hipposideridae,
549 Miniopteridae, Pteropodidae, and Rhinolophidae), each with similar propotions of
550 parasitized to non-parasitzed individuals (see Table 1). For haemosporidian-associated
551 tests, only the family Miniopteridae was analyzed, due to highly imbalanced prevalence or
552 sample sizes across all other families (Table 1). Dispersion estimates and fit tests were
553 implented using default DESeq2 parameters. False discovery rate (FDR) was calculated
554 using the Benjamini-Hochberg method for each of the bat families analyzed, and *p*-
555 values were adjusted accordingly.
556
557 ACKNOWLEDGMENTS
558
559 We thank the Kenya Wildlife Service and the Uganda Wildlife Authority for permission
560 to conduct research in national parks. For logistical support and assistance in the field, we
561 thank Mike Bartonjo of the National Museums of Kenya, Phausia Kweyu of Karatina
562 University, Dr. Robert Kityo, Solomon Sebuliba, and Cissy Akoth of the Makerere
563 University Zoological Museum, Drs. Brian Amman, Jonathan Towner, and Rebecca
564 Tiller of the Centers for Disease Control and Prevention, and Lauren Lutz. We thank
565 Neil Gottel for his knowledge and assistance with laboratory processing of microbial
566 samples, and other members of the Gilbert Lab, including Alyson Yee, Cesar Cardona,

Thomas Kuntz, Drs. Bea Penalver, Melissa Dsouza, and Naseer Sangwan for the assistance with bacterial 16s analyses.

AUTHOR CONTRIBUTIONS

H.L.L. designed the research and wrote the first draft; H.L.L., E.W.J. analyzed data; T.C.D. produced bat phylogeny; H.L.L., P.W.W., W.B.S., J.C.K. conducted field research; J.A.G., B.D.P. provided funding and research support; all authors contributed to writing.

REFERENCES

1. Human Microbiome Project C (2012) Structure, function and diversity of the healthy human microbiome. *Nature* 486(7402):207-214.
2. Thaiss CA, Zmora N, Levy M, & Elinav E (2016) The microbiome and innate immunity. *Nature* 535(7610):65-74.
3. Nishida AH & Ochman H (2018) Rates of gut microbiome divergence in mammals. *Mol Ecol* 27(8):1884-1897.
4. Moeller AH*, et al.* (2014) Rapid changes in the gut microbiome during human evolution. *Proc Natl Acad Sci U S A* 111(46):16431-16435.
5. Kundu P, Blacher E, Elinav E, & Pettersson S (2017) Our Gut Microbiome: The Evolving Inner Self. *Cell* 171(7):1481-1493.
6. Li X*, et al.* (2017) Composition of Gut Microbiota in the Gibel Carp (Carassius auratus gibelio) Varies with Host Development. *Microb Ecol* 74(1):239-249.
7. Kolodny o*, et al.* (2017).
8. McFall-Ngai M*, et al.* (2013) Animals in a bacterial world, a new imperative for the life sciences. *Proc Natl Acad Sci U S A* 110(9):3229-3236.
9. Kwiatkowski DP (2005) How malaria has affected the human genome and what human genetics can teach us about malaria. *Am. J. Hum. Genet.* 77:171-190.
10. Dittmar K, Morse, Solo F., Dick, Carl W., Patterson, Bruce D. (2015) Bat fly evolution from the Eocene to the present (Hippoboscoidea, Streblidae and Nycteribiidae). *Parasite Diversity and Diversification: Evolutionary Ecology Meets Phylogenetics*, ed S. Morand BRK, D. T. J. Littlewood (Cambridge University Press, Cambridge, U. K.).

602 11. Dick CW, Patterson, B. D. (2006) *Micromammals and Macroparasites: From*
603 *Evolutionary Ecology to Management* (Springer, Kato Bunmeisha, Japan).
604 12. Schaer J*, et al.* (2013) High diversity of West African bat malaria parasites
605 and a tight link with rodent Plasmodium taxa. *Proceedings of the National*
606 *Academy of Sciences* 100:17415-17419.
607 13. Lutz HL*, et al.* (2016) Diverse sampling of East African haemosporidians
608 reveals chiropteran origin of malaria parasites in primates and rodents. *Mol*
609 *Phylogenet Evol* 99:7-15.
610 14. Towner JS*, et al.* (2009) Isolation of genetically diverse Marburg viruses from
611 Egyptian fruit bats. *PLoS Pathog* 5(7):e1000536.
612 15. Olival KJ & Hayman DT (2014) Filoviruses in bats: current knowledge and
613 future directions. *Viruses* 6(4):1759-1788.
614 16. Amman BR*, et al.* (2015) A Recently Discovered Pathogenic Paramyxovirus,
615 Sosuga Virus, is Present in Rousettus aegyptiacus Fruit Bats at Multiple
616 Locations in Uganda. *J Wildl Dis* 51(3):774-779.
617 17. Li W*, et al.* (2005) Bats are natural reservoirs of SARS-like coronaviruses.
618 *Science* 310:676-679.
619 18. Chua KB*, et al.* (2002) Isolation of Nipah virus from Malaysian island flying-
620 foxes. *Microbes and Infection* 4:145-151.
621 19. Amir A*, et al.* (2017) Deblur Rapidly Resolves Single-Nucleotide Community
622 Sequence Patterns. *mSystems* 2(2).
623 20. Sturgeon A, Pinder SL, Costa MC, & Weese JS (2014) Characterization of the
624 oral microbiota of healthy cats using next-generation sequencing. *Vet J*
625 201(2):223-229.
626 21. Ley RE*, et al.* (2008) Evolution of mammals and their gut microbes. *Science*
627 320(5883):1647-1651.
628 22. Mark Welch JL, Rossetti BJ, Rieken CW, Dewhirst FE, & Borisy GG (2016)
629 Biogeography of a human oral microbiome at the micron scale. *Proc Natl*
630 *Acad Sci U S A* 113(6):E791-800.
631 23. Brix L, Hansen MJ, Kelly A, Bertelsen MF, & Bojesen AM (2015) Occurrence of
632 Pasteurellaceae Bacteria in the Oral Cavity of the Tasmanian Devil
633 (Sarcophilus Harrisii). *J Zoo Wildl Med* 46(2):241-245.
634 24. Grice EA & Segre JA (2011) The skin microbiome. *Nat Rev Microbiol* 9(4):244-
635 253.
636 25. Ursell LK*, et al.* (2012) The interpersonal and intrapersonal diversity of
637 human-associated microbiota in key body sites. *J Allergy Clin Immunol*
638 129(5):1204-1208.
639 26. Costello EK*, et al.* (2009) Bacterial community variation in human body
640 habitats across space and time. *Science* 326(5960):1694-1697.
641 27. Chiarello M, Villéger, S., Bouvier, C., Bettarel, Y., Bouvier, T. (2015) High
642 diversity of skin-associated bacterial communities in marine fishes is
643 promoted by their high variability among body parts, individuals and species.
644 *FEMS Microbiol Ecol* 91(7):1-12.
645 28. Caviedes-Vidal E, McWhorter, T. J., Lavin, S. R., Chediak, J. G., Tracy, C. R.,
646 Karasov, W. H. (2007) The digestive adaptation of flying vertebrates: High

647 intestinal paracellular absorption compensates for smaller guts. *PNAS*
648 104(48):19132-19137.
649 29. Price ER, Brun A, Caviedes-Vidal E, & Karasov WH (2015) Digestive
650 adaptations of aerial lifestyles. *Physiology (Bethesda)* 30(1):69-78.
651 30. Caviedes-Vidal E*, et al.* (2008) Paracellular absorption: a bat breaks the
652 mammal paradigm. *PLoS One* 3(1):e1425.
653 31. Moeller AH, Car-Qintero, A., Mjungu, D., Georgiev, A. V., Lonsdorf, E. V., Muller,
654 M. N., Pusey, A. E., Peeters, M., Hahn, B. H., Ochman, H. (2016) Cospeciation of
655 gut microbiota with hominids. *Science* 353(6297):380-382.
656 32. Sanders JG*, et al.* (2015) Baleen whales host a unique gut microbiome with
657 similarities to both carnivores and herbivores. *Nat Commun* 6:8285.
658 33. Moeller AH*, et al.* (2017) Dispersal limitation promotes the diversification of
659 the mammalian gut microbiota. *Proc Natl Acad Sci U S A* 114(52):13768-
660 13773.
661 34. Thomas T*, et al.* (2016) Diversity, structure and convergent evolution of the
662 global sponge microbiome. *Nat Commun* 7:11870.
663 35. Avena CV*, et al.* (2016) Deconstructing the Bat Skin Microbiome: Influences
664 of the Host and the Environment. *Front Microbiol* 7:1753.
665 36. Muletz Wolz CR, Yarwood SA, Campbell Grant EH, Fleischer RC, & Lips KR
666 (2018) Effects of host species and environment on the skin microbiome of
667 Plethodontid salamanders. *J Anim Ecol* 87(2):341-353.
668 37. Bryant JA, Lamanna, C., Morlon, H., Kerkhoff, A. J., Enquist, B. J., Green, J. L.
669 (2008) Microbes and mountainsides: contrasting elevational patterns of
670 bacterial and plan diversity. *PNAS* 105:11505-11511.
671 38. Singh D*, et al.* (2014) Strong elevational trends in soil bacterial community
672 composition on Mt. Halla, South Korea. *Soil Biology and Biochemistry* 68:140-
673 149.
674 39. Carrillo-Araujo M*, et al.* (2015) Phyllostomid bat microbiome composition is
675 associated to host phylogeny and feeding strategies. *Front Microbiol* 6:447.
676 40. Phillips CD*, et al.* (2012) Microbiome analysis among bats describes
677 influences of host phylogeny, life history, physiology and geography. *Mol Ecol*
678 21(11):2617-2627.
679 41. Eckburg PB, Bik, E. M., Bernstein, C. N., Purdom, E., Dethlefsen, L., Sargent, M.,
680 Gill, S. R., Nelson, K. E., Relman, D. A. (2005) Diversity of human intestinal
681 microbial flora. *Science* 308(5728):1635-1638.
682 42. Yildirim S*, et al.* (2010) Characterization of the fecal microbiome from non-
683 human wild primates reveals species specific microbial communities. *PLoS*
684 *One* 5(11):e13963.
685 43. Bik EM*, et al.* (2016) Marine mammals harbor unique microbiotas shaped by
686 and yet distinct from the sea. *Nat Commun* 7:10516.
687 44. Gutman N, Hansen MJ, Bertelsen MF, & Bojesen AM (2016) Pasteurellaceae
688 bacteria from the oral cavity of Tasmanian devils (Sarcophilus Harrisii) show
689 high minimum inhibitory concentration values towards aminoglycosides and
690 clindamycin. *Lett Appl Microbiol* 62(3):237-242.
691 45. Verhulst NO*, et al.* (2011) Composition of human skin microbiota affects
692 attractiveness to malaria mosquitoes. *PLoS One* 6(12):e28991.

46. Busula AO, Takken W, JG DEB, Mukabana WR, & Verhulst NO (2017) Variation in host preferences of malaria mosquitoes is mediated by skin bacterial volatiles. *Med Vet Entomol* 31(3):320-326.
47. Verhulst NO*, et al.* (2009) Cultured skin microbiota attracts malaria mosquitoes. *Malar J* 8:302.
48. Robinson A*, et al.* (2018) Plasmodium-associated changes in human odor attract mosquitoes. *Proc Natl Acad Sci U S A* 115(18):E4209-E4218.
49. De Moraes CM*, et al.* (2014) Malaria-induced changes in host odors enhance mosquito attraction. *Proc Natl Acad Sci U S A* 111(30):11079-11084.
50. de Boer JG*, et al.* (2017) Odours of Plasmodium falciparum-infected participants influence mosquito-host interactions. *Sci Rep* 7(1):9283.
51. Song SJ, Amir, A., Metcalf, J. L., Amato, K. R., Xu, Z. Z., Humphrey, G., Knight, R. (2016) Preservation methods differ in fecal microbiome stability, affecting suitability for field studies. *mSystems* 1(3):1 - 12.
52. Caporaso JG, Lauber, C. L., Walters, W. A., Berg-Lyons, D., Lozupone, C. A., Turnbaugh, P. J., Fierer, N., Knight, R. (2011) Global patterns of 16S rRNA diversity at a depth of millions of sequences per sample. *PNAS* 108:4516-4522.
53. Caporaso JG*, et al.* (2012) Ultra-high-throughput microbial community analysis on the Illumina HiSeq and MiSeq platforms. *ISME J* 6(8):1621-1624.
54. Kozich JJ, Westcott, S. L., Baxter, N. T., Highlander, S. K., Schloss, P. D. (2013) Development of a dual-index sequencing strategy and curation pipeline for analyzing amplicon sequence data on teh MiSeq Illumina sequencing platform. *Applied and Environmental Microbiology* 79(17):5122-5120.
55. Caporaso JG, Kuczynski, J., Stombaugh, J., Bittinger, K., Bushman, F. D., Costello, E. K., Fierer, N., Gonzalez Peña, A., Goodrich, E. K., Gordon, J. I., Huttley, G. A., Kelley, S. T., Knights, D., Koenig, J. E., Ley, R. E., Lozupone, C. A., McDonald, D., Muegge, B. D., Pirrung, M., Reeder, J., Sevinsky, J. R., Turnbaugh, P. J., Walters, W. A., Widmann, J., Yatsunenko, T., Zaneveld, J., Knight, R. (2010) QIIME allows analysis of high-throughput community sequencing data. *Nature Methods* 7(5):335 - 336.
56. Rognes T, Flouri T, Nichols B, Quince C, & Mahe F (2016) VSEARCH: a versatile open source tool for metagenomics. *PeerJ* 4:e2584.
57. McMurdie PJ, Holmes, S. (2014) Waste not, want not: Why rarefying microbiome data is inadmissable. *PLoS Comput Biol* 10(4):1-12.
58. McMurdie PJ & Holmes S (2013) phyloseq: an R package for reproducible interactive analysis and graphics of microbiome census data. *PLoS One* 8(4):e61217.
59. Oksanen J.*, et al.* (2018) vegan: Community Ecology Package), R package version 2.5-2.
60. Wickham H (2016) *ggplot2: Elegant Graphics for Data Analysis* (Springer-Verlag, New York, NY).
61. Wickham H, François R, Henry L, & Müller K (2018) dplyr: A Grammar of Data Manipulation), R package version 0.7.6.
62. Breiman L (2001) Random Forests. *Machine Learning* 45:5-32.

63. Kurtz ZD, *et al.* (2015) Sparse and compositionally robust inference of microbial ecological networks. *PLoS Comput Biol* 11(5):e1004226.
64. Cardona C (2017) CAVNet: Creation Analysis and Visualization of Networks).
65. Csardi G, Nepusz, T. (2006) The Igraph Software Package for Complex Network Research. *InterJournal, Complex Systems* 1695.
66. Love MI, Huber W, & Anders S (2014) Moderated estimation of fold change and dispersion for RNA-seq data with DESeq2. *Genome Biol* 15(12):550.

FIGURE LEGENDS

Figure 1. Sampling localities and elevation, grouped by county (see Table S1 for full locality information). Colors correspond to elevation, and white numbers and size of points correspond to number of bats collected.

Figure 2. Alpha diversity of amplicon sequence variants (ASVs) by anatomical sites, including (A) Observed richness, (B) Shannon index of diversity, (C) ASVs shared between anatomical sites. Asterisks indicate significant differences between groups (Dunn's Test, Bonferroni corrected p-value $p < 0.0001$).

Figure 3. Percent relative abundance of top 11 bacterial families identified in gut, oral, and skin microniomes of bats. Individual points represent the relative abundance of bacterial families within a single library. Results are faceted by anatomical site and arranged by host phylogenetic relationship. Bacterial families are colored according to

764 bacterial phylum. Number of libraries is indicated in the upper right-hand corner of each
765 plot.
766
767 Figure 4. Rate of microbiome divergence across phylogenetic distance of bats. Strengths of
768 correlations assessed by Mantel tests (10,000 permutations) of microbial community
769 dissimilarity (unweighted and weighted UniFrac) and patristic distances calculated from a
770 maximum likelihood hypothesis of bat species from this study. Asterisk indicates significant
771 correlation ($p<0.05$) as determined by Mantel test.
772
773 Figure 5. (A) Distribution of skin microbial network clusters for parasitized and non-
774 parasitized bats, grouped by bat family (asterisks indicate signifiance at $p < 0.005$,
775 Kruskal-Wallis) (B) Visualization of skin bacterial networks (based on Fruchterman-
776 Reingold algorithm); colored nodes correspond to unique clusters of co-occurring ASVs
777 within each network.
778
779 Figure 6. Log2fold change in relative abundance of skin-associated ASVs from the four
780 most-sampled bat families estimated with DESeq2. ASVs shown were found to be
781 significantly associated with ectoparasite status in bats based on analysis of negative
782 binomial distributions of relative abundance (Banjamini-Hochberg FDR corrected *p*-
783 value $p < 0.05$). Positive values correspond to ASVs found to be enriched on parasitized
784 bats, and negative values correspond to ASVs found to be enriched on non-parasitized
785 bats. Gray bars highlight ASVs in bacterial families that were enriched in parasitized bats
786 for three out of four bat families.

Supplemental Figures

Figure S1. Alpha diversity measures of data rarefied to a read depth of 10,000. A) Observed ASV richness across anatomical site; gut and oral microbial richness differeed significantly from skin microbial richness (Kruskal-Wallis chi-squared = 677.01, df = 2, p < 2.2e-16, Dunn's test), but did not differ significantly from each other. B) Density plots of Shannon Index (SI) by anatomical site; SI of skin microbial richness and evenness differed significantly from the SI of both gut and oral microbiomes, which did not differ from each other (Kruskal-Wallis chi-squared = 678.0885, df = 2, p < 2.2e-16, Dunn's test). C) Venn diagram of shared and specific ESVs across different anatomical sites. As with analyses of the non-rarefied data set, skin exhibited the high-est diversity (27,825 ASVs), followed by the oral microbiome (10,696 ASVs), and lastly the gut (6,492 ESVs). Rarefying data led to a loss of 1,079 ASVs (4% of total ASVs) that did not appear in any sample after rarefaction, and the removal of 1,079 libraries that had <10,000 reads. D) Mean ASV richness as read depth increases, with removal of libraries containing fewer than the identified number of reads (note - color key in D differs from color key in A-C).

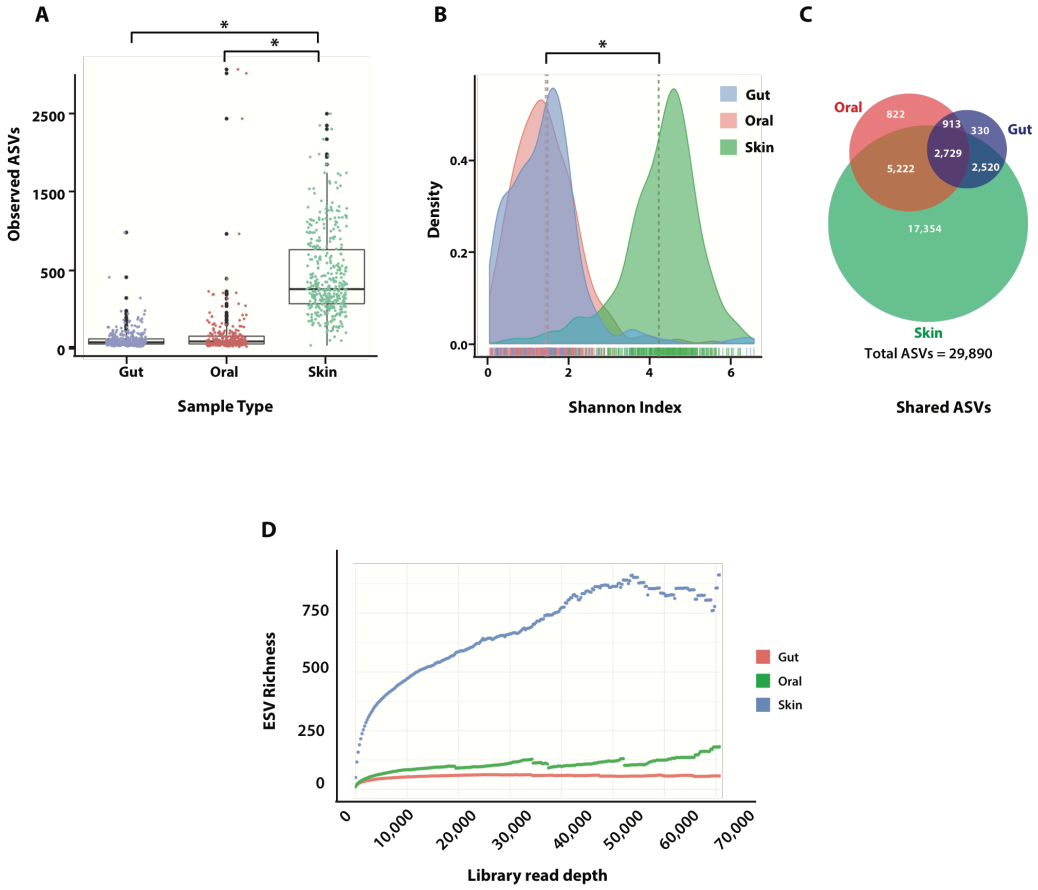

Figure S2. Intraspecific variation across anatomical sites measured as beta dispersion of (A) unweighted UniFrac, (B) weighted UniFrac, and (C) Bray-Curtis distances. Dotted lines indicate mean dispersion for anatomical groupings; numbers in parentheses indicate sample size per bat species. White and gray boxes correspond to the chiropteran suborders Yangochiroptera (microbats) and Yinpterochiroptera (fruits bats and kin), respectively.

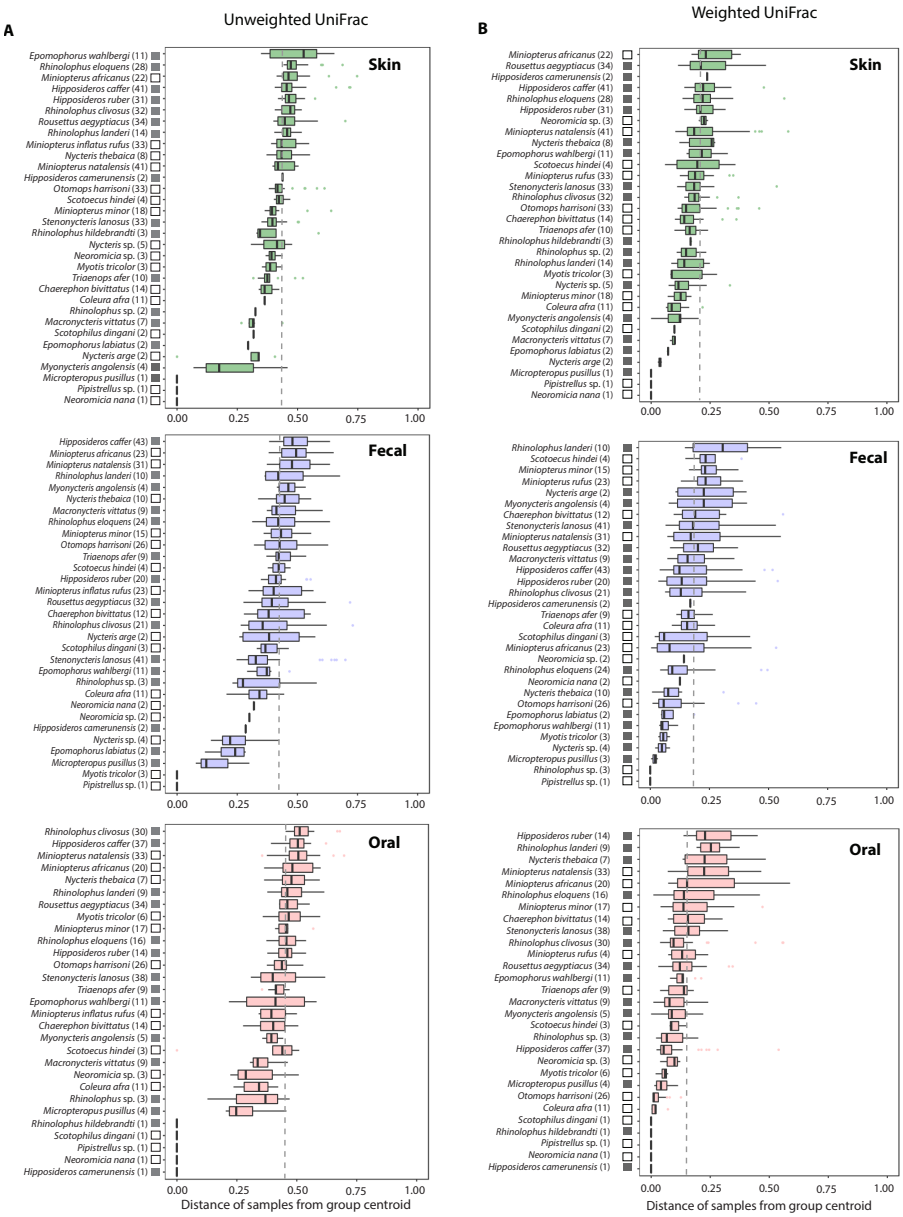

789

Figure S2 CONTINUED. Intraspecific variation across anatomical sites measured as beta dispersion of (A) unweighted UniFrac, (B) weighted UniFrac, and (C) Bray-Curtis distances. Dotted lines indicate mean dispersion for anatomical groupings; numbers in parentheses indicate sample size per bat species. White and gray boxes correspond to the chiropteran suborders Yangochiroptera (microbats) and Yinpterochiroptera (fruits bats and kin), respectively.

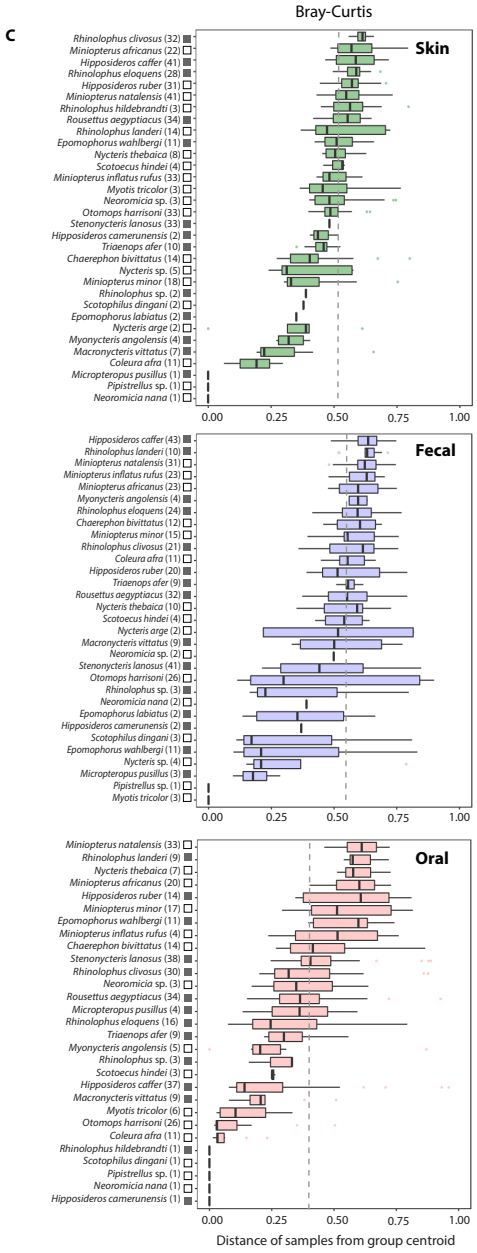

790

Figure S3. Linear regression of (A) Shannon diveristy and (B) observed ASV richness of gut, oral, and skin microbiomes against elevation from which host was sampled (~0 - 2500 meters above sea-level). R^2 and significance values are provided within each plot.

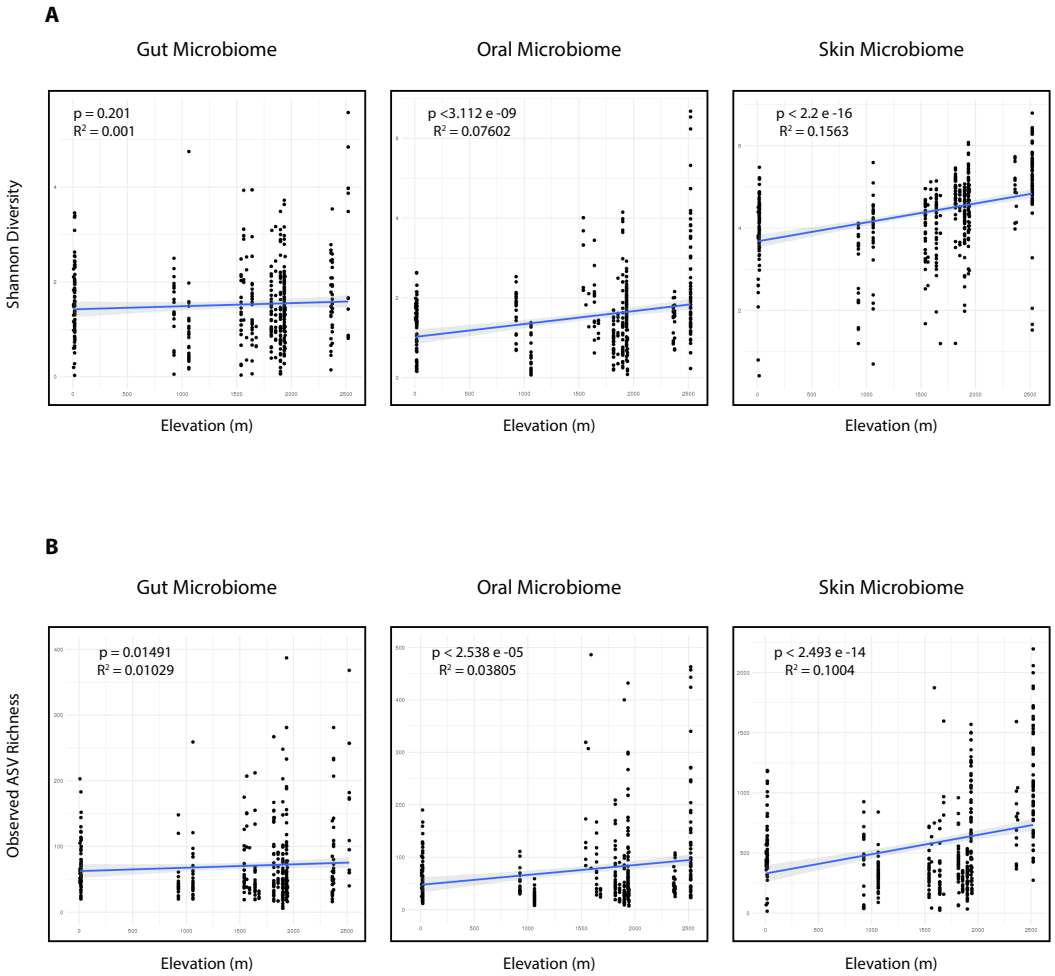

791

Figure S4. Network Analyses. A) Node degree dsitribution of parasitized and non-parasitized bats, grouped by family. B) Network fragility plots, showing natural network connectivity with sequential removal of nodes ordered by betweenness and degree.

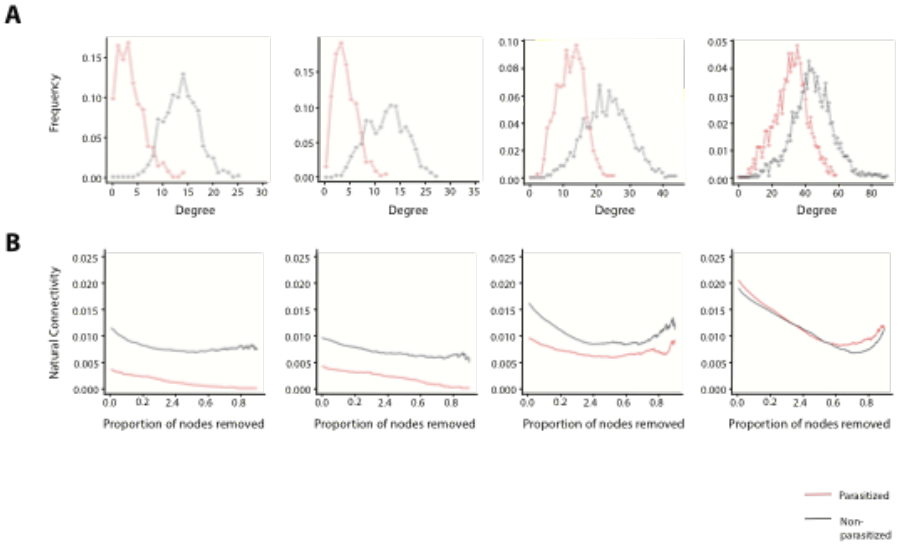

792

Figure S5. Maximum likelihood phylogeny of bat species based on the mitochondrial Cytochrome *b* locus (Cyt *b*). Phylogenetic distances were calculated as patristic distances based on maximum likelihood reconstruction of bat species-level phylogeny with 1000 bootstrap (bs) replicates. Closed black circles > 97% bs support, open circles > 70% bs support. Voucher specimens are accessioned at the Field Museum of Natural History (Chicago, IL); accession information can be found in Table S3 (where specimens included in phylogenetic analyses are highlighted in red).

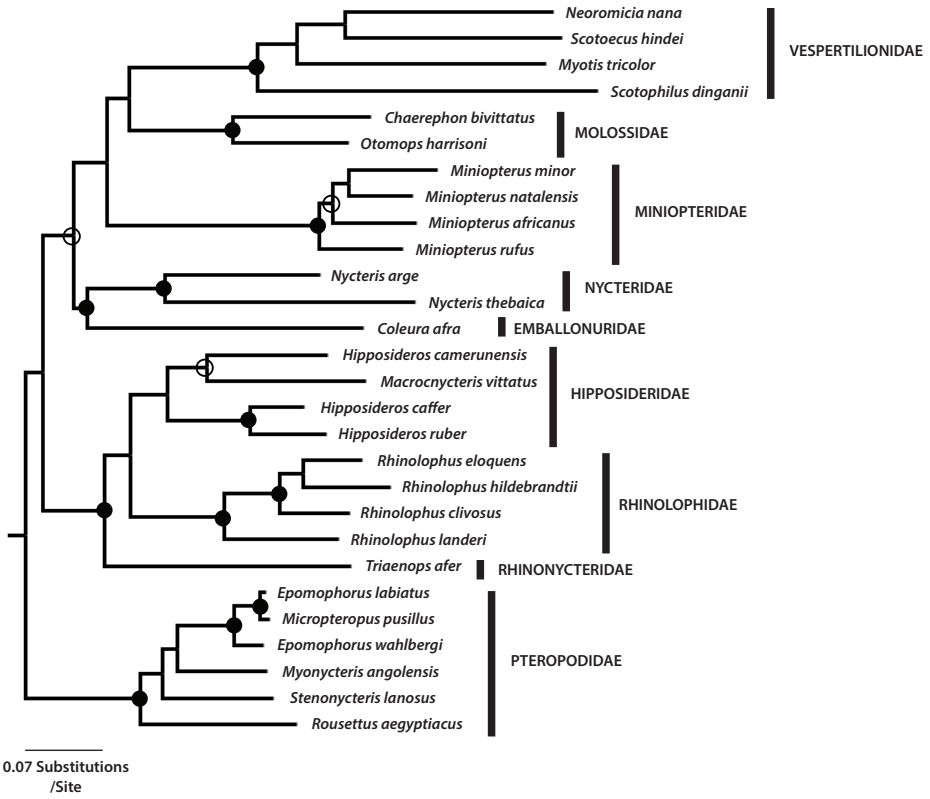

793